SNSN-XXX-XX
September 4, 2012

Search for *CP* Violation in the Decays $D^{\pm} \to K^0_S K^{\pm}$, $D^{\pm}_s \to K^0_S K^{\pm}$, and $D^{\pm}_s \to K^0_S \pi^{\pm}$

Riccardo Cenci
(on behalf of the *BABAR* collaboration)

University of Maryland, College Park, Maryland 20742, USA

We report on a search for *CP* violation in the decays $D^{\pm} \to K^0_S K^{\pm}$, $D^{\pm}_s \to K^0_S K^{\pm}$ and $D^{\pm}_s \to K^0_S \pi^{\pm}$ using a data set corresponding to an integrated luminosity of 469 fb^{-1} collected with the *BABAR* detector at the PEP-II asymmetric energy e^+e^- storage rings. The *CP*-violating decay rate asymmetries A_{CP} are determined to be $(+0.13 \pm 0.36(\text{stat}) \pm 0.25(\text{syst}))\%$, $(-0.05 \pm 0.23(\text{stat}) \pm 0.24(\text{syst}))\%$, and $(+0.6 \pm 2.0(\text{stat}) \pm 0.3(\text{syst}))\%$, respectively for the three modes, before correction for the relevant K^0_S asymmetry. After this correction, all the measurements are consistent with zero within one standard deviation. These are currently the most precise measurements of these asymmetries.

PRESENTED AT

Charm 2012
5$^{\text{th}}$ International Workshop on Charm Physics
Honolulu, Hawai'i, USA, May 14$^{\text{th}}$–17$^{\text{th}}$, 2012

1 Introduction

CP violation (CPV) in charm decay is a sensitive probe of physics beyond the Standard Model (SM). Owing to its suppression within the SM, a significant observation of direct CPV in charm decay would indicate the possible presence of new physics effects in the decay process. In a previous publication [1], we reported a precise measurement of CP asymmetry in the decay $D^{\pm} \to K^0_S\pi^{\pm}$, where the measured asymmetry was found to be consistent with the value expected for indirect CPV in the K^0 system. The LHCb and CDF collaborations have recently reported evidence for CPV in the decays $D^0 \to K^+K^-$ and $D^0 \to \pi^+\pi^-$ [2, 3], which, if confirmed, could be due either to new physics effects or to significant enhancement of penguin diagrams in charm decays [4, 5]. Additional information and corroboration of these observations in other channels are necessary to resolve these questions.

In this report we present measurements of direct CPV asymmetries in the decay channels: $D^{\pm} \to K^0_SK^{\pm}$, $D^{\pm}_s \to K^0_SK^{\pm}$, and $D^{\pm}_s \to K^0_S\pi^{\pm}$. For these channels, as in the case of the decay $D^{\pm} \to K^0_S\pi^{\pm}$, we expect a K^0-induced asymmetry of $\approx (\pm 0.332 \pm 0.006)\%$ [6]. The sign of the K^0-induced asymmetry is positive (negative) if a K^0 ($\overline{K}^0$) is present in the corresponding tree level Feynman diagram. The exact magnitude of the asymmetry would depend on the requirements on the reconstructed $K^0_S \to \pi^+\pi^-$ decays and the decay kinematics [7]. Previous measurements of A_{CP} in these channels have been reported by the CLEO-c [8] and Belle collaborations [9].

For this analysis we employ a technique similar to that used in the measurement of CPV in $D^{\pm} \to K^0_S\pi^{\pm}$ [1], thus for the description of certain analysis details we refer to our previous publication.

2 Data Selection and Fit Procedure

The data used for these measurements were recorded at or near the $\Upsilon(4S)$ resonance by the *BABAR* detector at the PEP-II storage rings. The *BABAR* detector and the coordinate system used throughout are described in detail in Refs. [10, 11]. The total integrated luminosity used is 469 fb^{-1}. To avoid any potential biases in the measurements, we adopt a "blind analysis" approach, where for each channel we finalize the whole analysis procedure prior to extracting A_{CP} from the data.

Signal candidates were reconstructed by combining a K^0_S candidate reconstructed in the decay mode $K^0_S \to \pi^+\pi^-$ with a charged pion or kaon candidate. A K^0_S candidate is reconstructed from two oppositely charged tracks with assigned the charged-pion mass. K^0_S candidates are required to have an invariant mass within ± 10 MeV/c^2 of the nominal K^0_S mass [6], which is equivalent to slightly more than $\pm 2.5\,\sigma$ in the measured K^0_S mass resolution. The χ^2 probability of the $\pi^+\pi^-$ vertex fit must be greater than 0.1 %. To reduce combinatorial background, we require the measured

flight length of the K^0_S candidate to be greater than 3 times its uncertainty. A reconstructed charged-particle track that has $p_T \geq 400$ MeV/c is selected as a pion or kaon candidate, where p_T is the magnitude of the momentum in the plane perpendicular to the e^+e^- collision axis. At *BABAR*, charged hadron identification is achieved through measurements of specific ionization energy loss in the tracking system, and the Cherenkov angle obtained from a detector of internally reflected Cherenkov light. A CsI(Tl) electromagnetic calorimeter provides photon detection, electron identification, and neutral pion reconstruction [10]. In our measurement, it is required that a pion candidate not be identified as a kaon, a proton, or an electron, while a kaon candidate is required to be identified as a kaon and not as a pion, a proton, or an electron. The criteria used to select pion or kaon candidates are very effective in reducing the charge asymmetry from track reconstruction and identification, as inferred from the study of control samples, as described below. A kinematic vertex fit to the whole decay chain is then performed, and it is required that each candidate form a vertex close to the beam interaction region [12]. We retain only $D^\pm_{(s)}$ candidates having a χ^2 probability for this fit greater than 0.1%, and an invariant mass $m(K^0_S h), h = \pi, K$, within $\pm 65\,\mathrm{MeV}/c^2$ of the nominal $D^+_{(s)}$ mass [6]; this is equivalent to more than $\pm 8\,\sigma$ in the measured $D^\pm_{(s)}$ mass resolution.

We further require the magnitude of the $D^\pm_s$ candidate momentum in the e^+e^- center-of-mass (CM) system, $p^*(D^\pm_s)$, to be between 2.6 and 5.0 GeV/c to suppress the combinatorial background from $B\overline{B}$ events. For the decay channel $D^\pm \to K^0_S K^\pm$, which suffers from lower statistics, we retain candidates with $p^*(D^\pm)$ between 2.0 and 5.0 GeV/c. This selects some signal events originating from B meson decays [13], while maintaining an acceptable level of combinatorial background. Additional background rejection is obtained by requiring that the impact parameter of the $D^\pm_{(s)}$ candidate with respect to the e^+e^- interaction region [10], projected onto the plane perpendicular to the collision axis, be less than 0.3 cm, and that the $D^\pm_{(s)}$ lifetime $\tau_{xy}(D^\pm_{(s)})$ be between -15 and 35 ps. The lifetime is measured using $L_{xy}(D^\pm_{(s)})$, defined as the distance of the $D^\pm_{(s)}$ decay vertex from the interaction region projected onto the plane perpendicular to the collision axis.

In order to further optimize the sensitivity of the A_{CP} measurements, a multivariate algorithm is constructed from seven discriminating variables for each $D^\pm_{(s)}$ candidate. These are: $\tau_{xy}(D^\pm_{(s)})$, $L_{xy}(D^\pm_{(s)})$, $p^*(D^\pm_{(s)})$, the momentum magnitude and transverse component with respect to the beam axis for the K^0_S, and for the pion or kaon candidate. For $D^\pm \to K^0_S K^\pm$ and $D^\pm_s \to K^0_S K^\pm$ the multivariate algorithm with the best performance is a Boosted Decision Tree (BDT), while for $D^\pm_s \to K^0_S \pi^\pm$ the best algorithm is a Projective Likelihood (LH) method [14]. The final selection criteria, based on the output of the relevant multivariate selector, are optimized using the $S/\sqrt{S+B}$ ratio as defined in Ref. [1].

For each mode the signal yield is extracted using a binned maximum likelihood

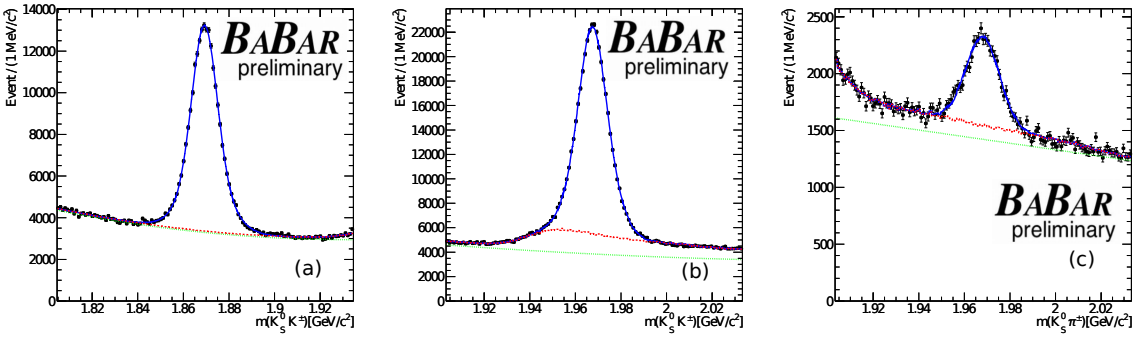

Figure 1: Invariant mass distribution for (a) $D^{\pm} \to K^0_S K^{\pm}$, (b) $D^{\pm}_s \to K^0_S K^{\pm}$, and (c) $D^{\pm}_s \to K^0_S \pi^{\pm}$ candidates from the data (black points). In each figure, the solid blue curve shows the fit to the data, the dashed red curve is the sum of all backgrounds, while the dotted green curve represents combinatorial background only.

(ML) fit to the distribution of invariant mass, $m(K^0_S h)$, for the selected $D^{\pm}_{(s)}$ candidates. The total probability density function (PDF) is the sum of signal and background components. The signal PDF is modeled as a sum of two Gaussian functions for both the $D^{\pm} \to K^0_S K^{\pm}$ and $D^{\pm}_s \to K^0_S K^{\pm}$ modes, and as a single Gaussian function for $D^{\pm}_s \to K^0_S \pi^{\pm}$ mode. The background PDF is taken as the sum of two components: background candidates from misidentified and partially reconstructed charm decays, and a combinatorial background component from other sources. For $D^{\pm} \to K^0_S K^{\pm}$ ($D^{\pm}_s \to K^0_S \pi^{\pm}$) the charm background is mainly from the tail of the invariant mass distribution of $D^{\pm}_s \to K^0_S K^{\pm}$ ($D^{\pm} \to K^0_S \pi^{\pm}$) candidates. For $D^{\pm}_s \to K^0_S K^{\pm}$ the charm background originates from $D^{\pm} \to K^0_S \pi^{\pm}$ where the $\pi^{\pm}$ is misidentified as $K^{\pm}$. This wrong mass assignment shifts the reconstructed invariant mass to higher values, and the resulting distribution is a broad peak with mean close to the $D^{\pm}_s$ mass. The charm background distributions are modeled using a PDF sampled from the simulation events for these modes. The combinatorial background is described as a first(second)-order polynomial for $D^{\pm}_s \to K^0_S \pi^{\pm}$ ($D^{\pm} \to K^0_S K^{\pm}$ and $D^{\pm}_s \to K^0_S K^{\pm}$). The fits to the $m(K^0_S h)$ distributions yield $(159.4 \pm 0.8) \times 10^3$ $D^{\pm} \to K^0_S K^{\pm}$ decays, $(288.2 \pm 1.1) \times 10^3$ $D^{\pm}_s \to K^0_S K^{\pm}$ decays, and $(14.33 \pm 0.31) \times 10^3$ $D^{\pm}_s \to K^0_S \pi^{\pm}$ decays. The data and the fits are shown in Fig. 1. All of the fit parameters are extracted from the fits to the data.

3 A_{CP} Asymmetry Extraction

For each channel, we determine A_{CP} by measuring the signal yield asymmetry A defined as:

$$A = \frac{N_{D^+_{(s)}} - N_{D^-_{(s)}}}{N_{D^+_{(s)}} + N_{D^-_{(s)}}}, \tag{1}$$

where $N_{D^+_{(s)}}$ ($N_{D^-_{(s)}}$) is the number of $D^+_{(s)}$($D^-_{(s)}$) decays determined from the mass fit. We consider A to be the result of two other contributions in addition to A_{CP}, namely the forward-backward (FB) asymmetry (A_{FB}) and a detector-induced component. We measure A_{FB} together with A_{CP} using the selected dataset, while we correct the data for the detector-induced component using coefficients from a control sample.

In this analysis we use a data-driven method, described in detail in Ref. [1], to determine the charge asymmetry in track reconstruction as a function of the magnitude of the track momentum and its polar angle. The method exploits the fact that the $\Upsilon(4S) \to B\overline{B}$ events provide sample of evenly populated positive and negative tracks, free of any physics-induced asymmetries, hence allowing the determination of detector-related asymmetries in the reconstruction of charged-particle tracks. Starting from a sample of 50.6 fb^{-1} of data collected at the $\Upsilon(4S)$ resonance and an off-resonance data set of 44.8 fb^{-1}, we obtain a large sample of charged tracks and apply the same charged pion or kaon track selection criteria used in the reconstruction of $D^\pm_{(s)} \to K^0_S K^\pm$ and $D^\pm_s \to K^0_S \pi^\pm$ decays. Then, by subtracting the off-resonance sample from the on-resonance sample, we obtain a sample of more than 120 million pion candidates and 40 million kaon candidates, originating from $\Upsilon(4S)$ decays. These are then used to compute the efficiency ratios for positive and negative kaons and pions. The ratio values and associated statistical errors are shown in Fig. 2. For $D^-_{(s)} \to K^0_S K^-$ ($D^-_s \to K^0_S \pi^-$) decays, the $D^-_{(s)}$ (D^-_s) yields, in intervals of kaon (pion) momentum and $\cos\theta$, are weighted with the kaon (pion) efficiency ratios to correct for the detection efficiency differences between K^+ and K^- (π^+ and π^-), leaving only FB and *CP* asymmetries. The largest correction is around 1% for pions and 2% for kaons.

Neglecting the second-order terms that contain the product of A_{CP} and A_{FB}, the resulting asymmetry can be expressed simply as the sum of the two. Given that A_{FB} is an odd function of $\cos\theta^*_D$, where θ^*_D is the polar angle of the $D^\pm_{(s)}$ candidate momentum in the e^+e^- CM frame, A_{CP} and A_{FB} can be written as a function of $|\cos\theta^*_D|$ as follows:

$$A_{FB}(|\cos\theta^*_D|) = \frac{A(+|\cos\theta^*_D|) - A(-|\cos\theta^*_D|)}{2} \tag{2}$$

and

$$A_{CP}(|\cos\theta^*_D|) = \frac{A(+|\cos\theta^*_D|) + A(-|\cos\theta^*_D|)}{2}, \tag{3}$$

where $A(+|\cos\theta^*_D|)$ is the measured asymmetry for the $D^\pm_{(s)}$ candidates in a positive $\cos\theta^*_D$ bin and $A(-|\cos\theta^*_D|)$ in its negative counterpart.

A simultaneous Maximum Likelihood (ML) fit to the $D^+_{(s)}$ and $D^-_{(s)}$ invariant mass distributions is carried out to extract the signal yield asymmetries for each one of the

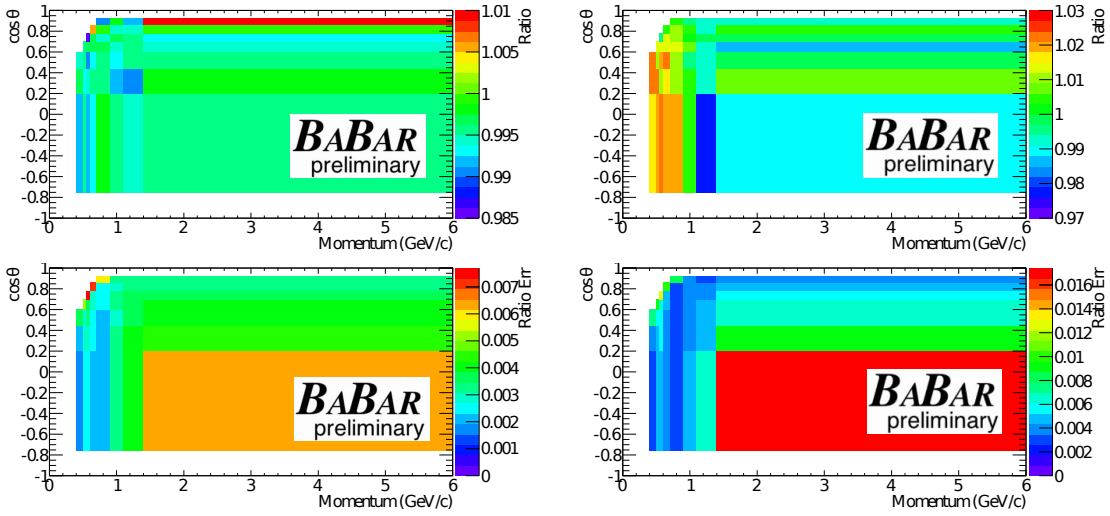

Figure 2: Ratio between the detection efficiency for positive and negative tracks (top) and corresponding statistical errors (bottom). Plots on the left are for π^+ and π^-, while on the right for K^- and K^+. The values are computed using the numbers of positive and negative tracks in the selected control sample.

ten equal intervals of $\cos\theta^*_D$, starting with interval 0 defined as $-1.0 \geq \cos\theta^*_D \geq -0.8$. The PDF shape that describes the distribution in each sub-sample is the same as that used in the fit to the full sample, but the following parameters are allowed to float separately in each sub-sample (referred to below as split parameters): the yields for signal, charm background and combinatorial candidates; the asymmetries for signal and combinatorial candidates; the width and the fraction of the Gaussian function with largest contribution to the signal PDF; the first order coefficient for the polynomial of the combinatorial background. For $D^\pm \to K^0_S K^\pm$ the yield of charm background candidates has been fixed to 0 in intervals 0, 1, and 2 in order to obtain a fully converging fit. Interval 9 has the lowest number of candidates compared to the other intervals, so, for $D^\pm \to K^0_S K^\pm$ and $D^\pm_s \to K^0_S K^\pm$, we use only one Gaussian function in this interval for the signal PDF by fixing the fraction of the first Gaussian function to 1. For the CPV asymmetry of charm background candidates we use the same floating parameters as for the signal candidates, because the largest source of CPV asymmetry for both samples is the CPV contribution from $K^0 - \overline{K}^0$ mixing. For the mode $D^\pm_s \to K^0_S \pi^\pm$, where the primary charm background channel, $D^\pm \to K^0_S \pi^\pm$, has the same magnitude but opposite sign asymmetry from $K^0 - \overline{K}^0$ mixing, we use a separate parameter for the asymmetry of the charm background candidates. If the fit values for a split parameter are statistically compatible between two or more sub-samples, the parameter is forced to have the same floating value among those sub-samples only, in order to achieve a more stable fit. For $D^\pm_s \to K^0_S \pi^\pm$ the width of the first Gaussian function for the signal PDF is set to the same floating value

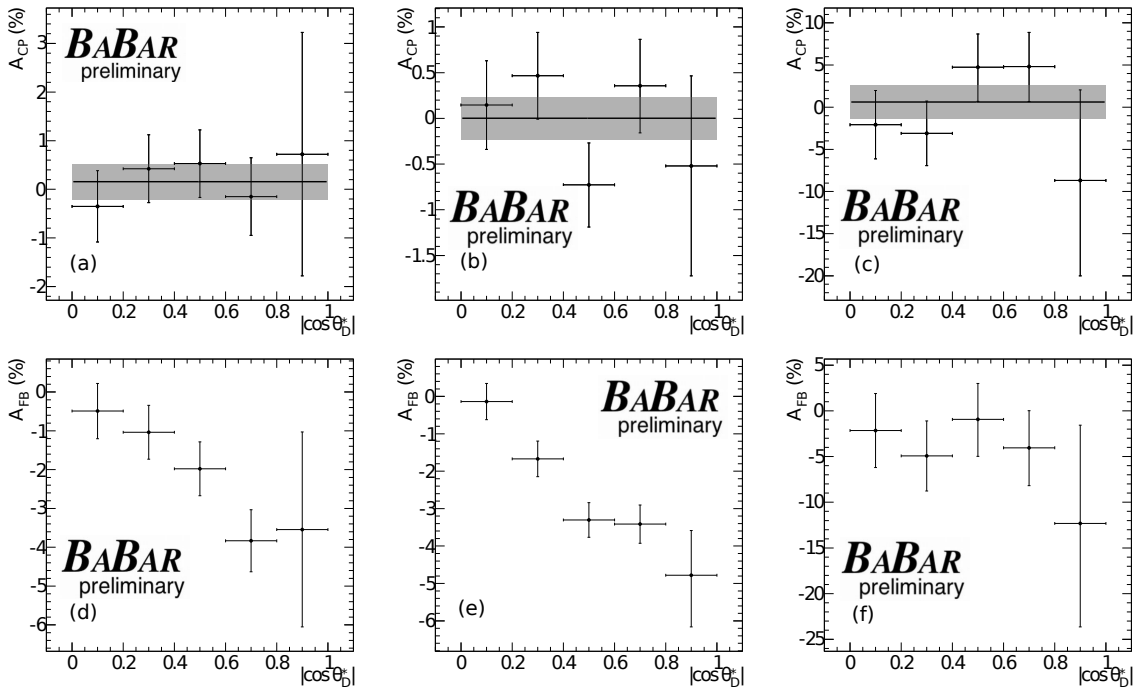

Figure 3: A_{CP} asymmetry for (a) $D^\pm \to K^0_S K^\pm$, (b) $D^\pm_s \to K^0_S K^\pm$, and (c) $D^\pm_s \to K^0_S \pi^\pm$ as a function of $|\cos\theta^*_D|$ in the data sample. The solid line represents the central value of A_{CP} and the gray region is the $\pm 1\,\sigma$ interval, both obtained from a χ^2 minimization assuming no dependence on $|\cos\theta^*_D|$. The corresponding A_{FB} asymmetries are shown in (d), (e), and (f).

for intervals 0, 1, 2, and 3. The first order coefficient of the polynomial describing the combinatorial background is set to the same floating value for intervals 3 to 7 ($D^\pm \to K^0_S K^\pm$), for intervals 4 to 7 ($D^\pm_s \to K^0_S K^\pm$), and for intervals 1 to 6 ($D^\pm_s \to K^0_S \pi^\pm$). The final fits for $D^\pm \to K^0_S K^\pm$, $D^\pm_s \to K^0_S K^\pm$, and $D^\pm_s \to K^0_S \pi^\pm$ involve a total of 70, 80 and 64 free parameters, respectively.

The A_{CP} and A_{FB} values are shown in Fig. 3. The weighted average of the five A_{CP} values is found to be: $(0.16 \pm 0.36)\%$ for $D^\pm \to K^0_S K^\pm$, $(0.00 \pm 0.23)\%$ for $D^\pm_s \to K^0_S K^\pm$, and $(0.6 \pm 2.0)\%$ for $D^\pm_s \to K^0_S \pi^\pm$, where the errors are statistical only.

4 Analysis Validation and Systematics

We perform two tests to validate the analysis procedure for each channel. The first involves generating 5000 toy MC experiments using the PDF obtained from the fit to data, and then extracting A_{CP} from each experiment. For the modes $D^\pm \to K^0_S K^\pm$ and $D^\pm_s \to K^0_S K^\pm$, we find small biases of -0.036 ± 0.014 and $+0.041 \pm 0.014$ (in

Table 1: Summary of the systematic error contributions to the A_{CP} measurement in each mode. The values are given as absolute percentage (*BABAR* Preliminary).

Systematic uncertainty [%]	$D^{\pm} \to K^0_S K^{\pm}$	$D^{\pm}_s \to K^0_S K^{\pm}$	$D^{\pm}_s \to K^0_S \pi^{\pm}$
Efficiency of PID selectors	0.05%	0.05%	0.05%
Statistics of the control sample	0.23%	0.23%	0.06%
Mis-identified tracks in the control sample	0.01%	0.01%	0.01%
Binning in $\cos\Theta$	0.04%	0.02%	0.27%
$K^0 - \overline{K}^0$ regeneration	0.05%	0.05%	0.06%
$K^0_S - K^0_L$ interference	0.015%	0.014%	0.008%
Total	0.25%	0.24%	0.29%

units of statistical error), in the fitted values of the A_{CP} parameter. Therefore we apply a systematic correction of +0.013% to the value of A_{CP} for $D^{\pm} \to K^0_S K^{\pm}$ and of -0.01% to that for $D^{\pm}_s \to K^0_S K^{\pm}$, to account for this effect. The fit returns an accurate estimate of the statistical uncertainty for all the modes. The second test involves fitting a large number of MC events from the full *BABAR* detector simulation. We measure A_{CP} from this MC sample to be within $\pm 1\,\sigma$ of the generated value of zero.

A list of systematic error contributions and the quadrature sum for each mode is reported in Table 1. Primary sources of systematic uncertainty are the statistical uncertainties in the detection efficiency ratios used to weight the $D^{\pm}_{(s)}$ yields and the contributions from misidentified particles in the data control sample used to determine the charge asymmetry in track reconstruction efficiency.

The technique used here to remove the charge asymmetry from detector-induced effects produces a small systematic uncertainty in the measurement of A_{CP} due to the statistical error on the relative efficiency estimation. We perform simultaneous fits to 500 samples of selected $D^{\pm}_s \to K^0_S K^{\pm}$ candidates where the applied corrections are smeared according to their errors, to produce a distribution of the deviations of A_{CP} values from the nominal one. The standard deviation of this distribution is 0.23%, and it is assigned as systematic uncertainty to the $D^{\pm}_s \to K^0_S K^{\pm}$ and $D^{\pm} \to K^0_S K^{\pm}$ modes, because this contribution depends only on the type of charged particle in the mode itself. For the $D^{\pm}_s \to K^0_S \pi^{\pm}$ mode we assign a systematic error contribution obtained as in Ref. [1]. This is the dominant source of systematic uncertainty for the $D^{\pm}_{(s)} \to K^0_S K^{\pm}$ modes, as shown in Table 1.

The small fraction of mis-identified particles in the generic track sample can introduce small biases in the estimation of the efficiencies, and subsequently in the A_{CP} measurements. Because of the good agreement between data and MC samples, we can use the MC-simulated candidates to measure the shift in the A_{CP} value from the fit

when the corrections are, or are not, applied. Again, this contribution depends only on the type of charged-particle track, hence for the $D_s^\pm \to K_S^0\pi^\pm$ mode we assume the same shift as that obtained in Ref. [1], namely +0.05%. Fitting the $D_s^\pm \to K_S^0 K^\pm$ MC sample when the corrections are, or are not, applied, we obtain a shift of +0.05%, and we assume this same uncertainty for the $D_s^\pm \to K_S^0 K^\pm$ and $D^\pm \to K_S^0 K^\pm$ modes. As a result, for each mode we shift the measured A_{CP} value by the net systematic shift to correct for this bias, and then, conservatively, include the same value as a contribution to the systematic uncertainty.

Using MC simulation, we evaluate an additional systematic uncertainty of $\pm 0.01\%$ due to a possible charge asymmetry present in the control sample before applying the selection criteria. Another systematic uncertainty from the simultaneous ML fit is due to the choice of interval-size in $\cos\theta_D^*$. This can be estimated using the largest A_{CP} deviation when the fit is performed using 8 or 12 intervals of $|\cos\theta_D^*|$, instead of 10. This is the dominant source of systematic uncertainty for the $D_s^\pm \to K_S^0\pi^\pm$ mode, as shown in Table 1.

We also consider a possible systematic uncertainty due to the regeneration of neutral kaons in the material of the detector, since K^0 and $\overline{K}^0$ mesons produced in the decay process can interact with the material in the tracking volume before they decay. Following a method similar to that described in Ref. [15], we compute the probability for a K^0 or $\overline{K}^0$ to interact inside the *BABAR* tracking system, and estimate an associated systematic uncertainty of $0.05 - 0.06\%$.

Another systematic contribution can be generated by the interference between the amplitudes of intermediate K_S^0 and K_L^0, because we are reconstructing our K_S^0 using $K_S^0 \to \pi^+\pi^-$, which is not a pure K_S^0 amplitude [7]. The bias in the asymmetry contribution induced by K^0–$\overline{K}^0$ mixing depends directly on the K_S^0 reconstruction efficiency as a function of the K_S^0 proper time and, approximately, the more the efficiency is not constant, the larger becomes the bias. We produce the K_S^0 reconstruction efficiency distribution as a function of the proper time using MC truth-matched events after the full selection. Then, following the method in Ref. [7], we estimate the asymmetry correction factor ΔA_{CP} defined as:

$$\Delta A_{CP} = A_{CP}^{\rm corr} - A_{CP}^{\rm fit}, \tag{4}$$

where $A_{CP}^{\rm fit}$ is the value obtained from the fit and $A_{CP}^{\rm corr}$ is the corrected value. The correction factors are reported in Table 2 and, to be conservative, we include their absolute values as a contribution to the systematic uncertainty. In a similar mode, we also estimate the correction factor for $D^\pm \to K_S^0\pi^\pm$ mode using the K_S^0 reconstruction efficiency distribution after the selection detailed in Ref. [1] and we find a value of +0.002%. All these corrections are rather small, even compared to those estimated in a similar analysis [16]. The smaller values of the corrections in this analysis are due to the improved efficiency for K_S^0 mesons with short decay times that we obtain

Table 2: Summary table for A_{CP} measurements. Uncertainties, where reported, are first statistical, and second systematic (*BABAR* Preliminary).

	$D^{\pm} \to K^0_S K^{\pm}$	$D^{\pm}_s \to K^0_S K^{\pm}$	$D^{\pm}_s \to K^0_S \pi^{\pm}$
A_{CP} value from the fit	$(0.16 \pm 0.36)\%$	$(0.00 \pm 0.23)\%$	$(0.6 \pm 2.0)\%$
Bias Corrections			
Toy MC experiments	$+0.013\%$	-0.01%	$-$
PID selectors	-0.05%	-0.05%	-0.05%
$K^0_S - K^0_L$ interference	$+0.015\%$	$+0.014\%$	-0.008%
A_{CP} corrected value	$(0.13 \pm 0.36 \pm 0.25)\%$	$(-0.05 \pm 0.23 \pm 0.24)\%$	$(0.6 \pm 2.0 \pm 0.3)\%$
A_{CP} contribution from $K^0 - \overline{K}^0$ mixing	$(-0.332 \pm 0.006)\%$	$(-0.332 \pm 0.006)\%$	$(0.332 \pm 0.006)\%$
A_{CP} value (charm only)	$(0.46 \pm 0.36 \pm 0.25)\%$	$(0.28 \pm 0.23 \pm 0.24)\%$	$(0.3 \pm 2.0 \pm 0.3)\%$

by making a requirement on the decay length divided by its uncertainty rather than on the decay length alone.

5 Conclusions and Acknowledgements

In conclusion, we measure the direct *CP* asymmetry, A_{CP}, in $D^{\pm} \to K^0_S K^{\pm}$, $D^{\pm}_s \to K^0_S K^{\pm}$, and $D^{\pm}_s \to K^0_S \pi^{\pm}$ decays using approximately 159,000, 288,000, and 14,000 signal candidates, respectively. The measured A_{CP} value for each mode is reported in Table 2, where the first error is statistical and the second is systematic. In the last row of the table, we also report the A_{CP} values after subtracting the expected A_{CP} contribution in each mode due to $K^0 - \overline{K}^0$ mixing. These results are consistent with zero and with the SM prediction within one standard deviation.

We are grateful for the extraordinary contributions of our PEP-II colleagues in achieving the excellent luminosity and machine conditions that have made this work possible. The success of this project also relies critically on the expertise and dedication of the computing organizations that support *BABAR*. The collaborating institutions wish to thank SLAC for its support and the kind hospitality extended to them. This work is supported by the US Department of Energy and National Science Foundation, the Natural Sciences and Engineering Research Council (Canada), the Commissariat à l'Energie Atomique and Institut National de Physique Nucléaire et de Physique des Particules (France), the Bundesministerium für Bildung und Forschung and Deutsche Forschungsgemeinschaft (Germany), the Istituto Nazionale di Fisica Nucleare (Italy), the Foundation for Fundamental Research on Matter (The Netherlands), the Research Council of Norway, the Ministry of Education and Science of the Russian Federation, Ministerio de Ciencia e Innovación (Spain), and the Science and

Technology Facilities Council (United Kingdom). Individuals have received support from the Marie-Curie IEF program (European Union) and the A. P. Sloan Foundation (USA).

References

[1] P. del Amo Sanchez *et al.* (*BABAR* Collaboration), Phys. Rev. D **83**, 071103 (2011).

[2] R. Aaij *et al.* (LHCb Collaboration), Phys. Rev. Lett. **108**, 111602 (2012).

[3] T. Aaltonen *et al.* [CDF Collaboration], arXiv:1207.2158 [hep-ex].

[4] G. Isidori, J. F. Kamenik, Z. Ligeti and G. Perez, Phys. Lett. B **711**, 46 (2012).

[5] E. Franco, S. Mishima and L. Silvestrini, arXiv:1203.3131 [hep-ph].

[6] K. Nakamura *et al.* (Particle Data Group), J. Phys. G **37**, 075021 (2010).

[7] Y. Grossman and Y. Nir, JHEP **1204**, 002 (2012).

[8] S. Dobbs *et al.* (CLEO Collaboration), Phys. Rev. D **76**, 112001 (2007).

[9] B. R. Ko *et al.* (Belle collaboration), Phys. Rev. Lett. **104**, 181602 (2010).

[10] B. Aubert *et al.* (*BABAR* Collaboration), Nucl. Instr. Methods Phys. Res., Sect. A **479**, 1 (2002).

[11] W. Menges, IEEE Nucl. Sci. Symp. Conf. Rec. **5**, 1470 (2006).

[12] W. D. Hulsbergen, Nucl. Instrum. Meth. A **552**, 566 (2005).

[13] The contribution from *CP* violation in B decays from the Standard Model processes is estimated to be negligible.

[14] P. Speckmayer, A. Hocker, J. Stelzer and H. Voss, J. Phys. Conf. Ser. **219**, 032057 (2010).

[15] B. R. Ko *et al.*, arXiv:1006.1938 [hep-ex] (2010).

[16] J. P. Lees *et al.* (BABAR Collaboration), Phys. Rev. D **85**, 031102 (2012).